A detailed analysis of current-voltage characteristics of Au/perylene-monoimide/n-Si Schottky barrier diodes over a wide temperature range

Ö. F. Yüksel,[1,a)] M. Kuş,[2] N. Şimşir,[1] H. Şafak,[1] M. Şahin,[1] and E. Yenel[2]
[1]*Department of Physics, Faculty of Science, Selçuk University Campus, Konya 42075 Turkey*
[2]*Department of Chemical Engineering, Selçuk University Campus, Konya 42075 Turkey and Advanced Technology Research and Application Center, Selçuk University Campus, Konya 42075 Turkey*

(Received 2 February 2011; accepted 1 June 2011; published online 25 July 2011)

The current-voltage characteristics of Au/perylene-monoimide (PMI)/n-Si Schottky device have been investigated at a wide temperature range between 75 and 300 K in detail. The measured current-voltage (I-V) characteristics of the device show a good rectification behavior at all temperatures. The electronic parameters such as the ideality factor and the barrier height are determined from the experimental data using standard current-voltage analysis method and also temperature dependence of these parameters is analyzed. In addition to the standard analysis, using the Cheung and Cheung method, the series resistance and some other electrical properties are calculated for the device, and a good agreement is obtained between relevant diode parameters. It was observed that Au/PMI/n-Si Schottky diodes exhibit space charge limited (SCL) conduction at all temperatures. Therefore, we have analyzed this SCL current mechanism in more detail. From this analysis, several electronic parameters related with the SCL mechanism are determined, and it is found that Poole-Frenkel effect is dominant in reverse bias. © *2011 American Institute of Physics*. [doi:10.1063/1.3610394]

I. INTRODUCTION

The metal-semiconductor (MS) contacts are still widely investigated because of their present and potential applications in technology. As is well known, the electrical properties of an MS contact depend mainly on the interface states between metal and semiconductor and also on the material parameters. The control of these properties has great importance in many device applications. This control mechanism can be obtained in some different ways. For this purpose, as an alternative to the conventional MS contacts, recently organic materials have been used between metal and semiconductor. By many authors, it is reported that the properties of MS diode can be easily modified by using suitable organic material.[1–6]

The contact resistance of a MS diode can vary depending on the electronic parameters of the interface. Hence, it is quite important to understand the relationship between the structural characteristics of organic materials and metal/semiconductor interface. On the other hand, the device characteristics depend also on the anisotropy of transport properties in the organic films.[7] An efficient charge transfer across the metal-organic interface has a critical value for better device performance. One of the most important factors that governs the charge injection is the energy barrier to be surmounted by charge carriers crossing the interface.[8–10]

Many studies have been performed to control the electronic properties of Schottky diodes based on organic semiconductors and to determine the characteristic parameters of organic films.[11–14] Electrical and interface properties of Au/DNA/n-Si (Ref. 15) and boron-dispersed triethanolamine/p-Si organic-based structures[1] were investigated. The electrical characterization of the Al/new fuchsin/n-Si organic modified device were studied by Güllü *et al.*[16] The control and modification of the properties of metal/semiconductor and metal/insulator/metal junctions by organic semiconductor thin films have been carried out by Yakuphanoğlu *et al.*[17,18] In addition, Aydoğan *et al.*[7] have worked for the first time on the effects of a thin Orcein organic layer in MS contacts.

Perylene and its derivatives belong to the one of the most widely studied classes of organic semiconductors. These materials have been used in many applications such as photovoltaic solar cells,[19–25] laser dyes,[26,27] organic light-emitting diodes[28,29] and electro photography.[30,31]

In this work, we have fabricated an Au/perylene-monoimide (PMI)/n-Si Schottky barrier diode and investigated the effect of the use of an organic film on the modification of electrical properties of Si Schottky diode. For this aim, perylene-monoimide (PMI) organic semiconductor is formed on an n-Si wafer by a spin coating method and then a Schottky barrier diode is prepared on this structure. The current-voltage characteristics of this diode are measured at a wide temperature range and analyzed in detail.

II. EXPERIMENTAL PROCEDURES

In this study, we have used an n-type P-doped Si semiconductor wafer with (1 0 0) orientation, having 1.5 cm × 1.5 cm dimensions, 380 μm thickness, and 0.1–20 Ωcm resistivity. Before making contacts, the wafer was chemically cleaned

a)Author to whom correspondence should be addressed. Electronic mail: fyuksel@selcuk.edu.tr.

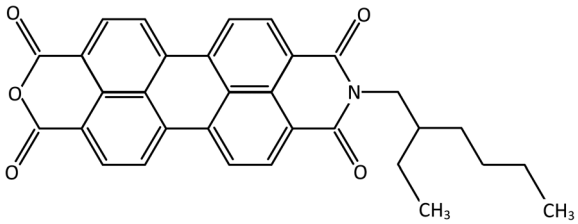

FIG. 1. Chemical representation of PMI.

using the Radio Corporation of America (RCA) cleaning procedure, i.e., a boil of 10 min in NH_3+H_2O_2+6 H_2O, followed by a 10 min boil in HCl+H_2O_2+6 H_2O with a final boil in diluted HF for 60 s. Then, the wafer was rinsed in de-ionized water of resistivity of 18.2 MΩcm with ultrasonic cleaning and dried by high-purity nitrogen. Immediately after surface cleaning, gold metal with a purity of 99.99% was thermally evaporated on the whole back surface of the wafer with a thickness of 1500 Å under vacuum of approximately 5×10^{-6} Torr. Then, a heat treatment was made at 500 °C for 3 min in vacuum to obtain a low resistivity ohmic contact. Next, a PMI organic film was formed by a spin coating method at a spinning rate of 1200 rpm with a Laurell Spin Coater. The chemical structure of PMI is given in Fig. 1. The PMI was synthesized according to the previously published procedures.[32–34] The thickness of film was measured to be approximately 150 nm by a Discrete Wavelength Ellipsometer TT-30. Then, Schottky contacts were deposited on this organic film with a diameter of 2 mm using a metal shadow mask by evaporating 99.99% purity gold metal with a thickness of 1500 Å in 5×10^{-6} Torr vacuum having an active area of A = 3.14 mm^2. The schematic representation of the device is shown in Fig. 2. The current-voltage (I-V) measurements were performed by a Keithley 2410 SourceMeter at a wide temperature range between 75 and 300 K using an ARS Closed Cycle Cryostat Model DE202 AI and a Lake Shore model 331 temperature controller.

III. RESULTS AND DISCUSSION

The most useful method to characterize the electrical properties of a MS contact is based on its I-V measurements. As is well known, the current of a diode can be given in the frame of thermionic emission model as[35–39]

$$I = I_0 \left[e^{\left(\frac{qV}{nkT}\right)} - 1 \right], \tag{1}$$

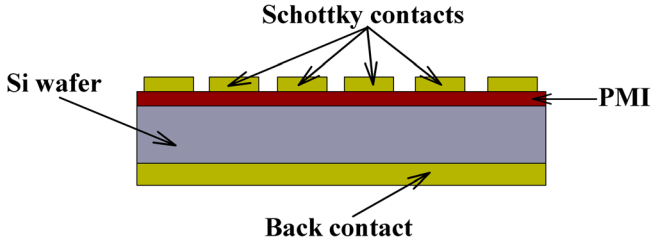

FIG. 2. (Color online) Cross-sectional view of Au/PMI/n-Si Schottky diode.

where

$$I_0 = AA^*T^2 e^{\left(-\frac{q\phi_{B0}}{kT}\right)} \tag{2}$$

is the saturation current. ϕ_{B0} is the effective barrier height at zero bias, A^* is the Richardson constant, A is the diode area, T is the temperature, q is the electron charge, V is the applied bias, n is the ideality factor, and k is the Boltzmann constant. The ideality factor n can be determined from the slope of linear region of the forward bias $\ln(I) - V$ characteristic as

$$n = \frac{q}{kT}\frac{dV}{dln(I)}. \tag{3}$$

For an ideal diode $n = 1$, but it is usually greater than unity for real diode structures. Actually, the ideality factor is a parameter indicating the Schottky barrier uniformity. In a more uniform interface structure, it has a value closer to the ideal case. On the other hand, the effective barrier height ϕ_{B0} can be obtained from Eq. (2) as

$$\phi_{B0} = \frac{kT}{q}\ln\left(\frac{AA^*T^2}{I_0}\right). \tag{4}$$

In Fig. 3, the current-voltage characteristics of Au/PMI/n-Si Schottky barrier diodes are plotted for a temperature range between 75 and 300 K. As shown in the figure, the Schottky contacts exhibit quite good diode behavior for all temperature values. By using Eqs. (3) and (4), we have determined the ideality factor n and the barrier height ϕ_{B0} values from the forward bias current-voltage characteristics for different temperatures. In the calculations, the diode area and the effective Richardson constant are taken as $A = 3.14\ mm^2$ and $A^* = 112\ AK^{-2}cm^{-2}$, respectively. The variations of n and ϕ_{B0} with temperature are plotted in Fig. 4. As seen from the figure, while the ideality factor decreases almost exponentially, the barrier height increases linearly with the temperature.

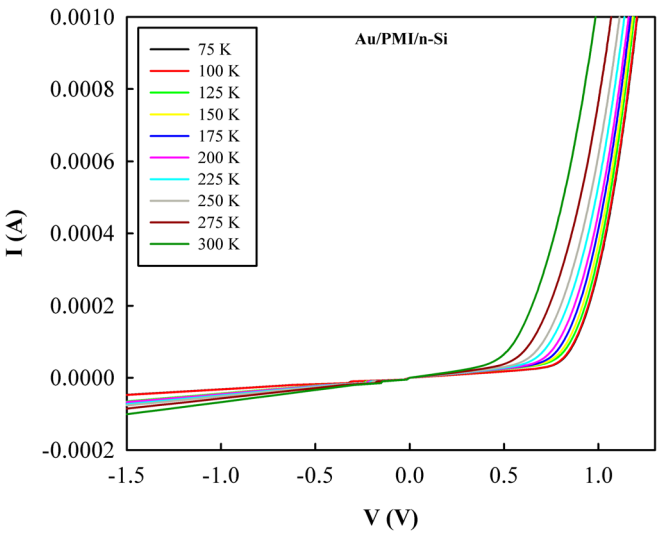

FIG. 3. (Color online) Current-voltage characteristics of Au/PMI/n-Si Schottky barrier diodes at various temperatures.

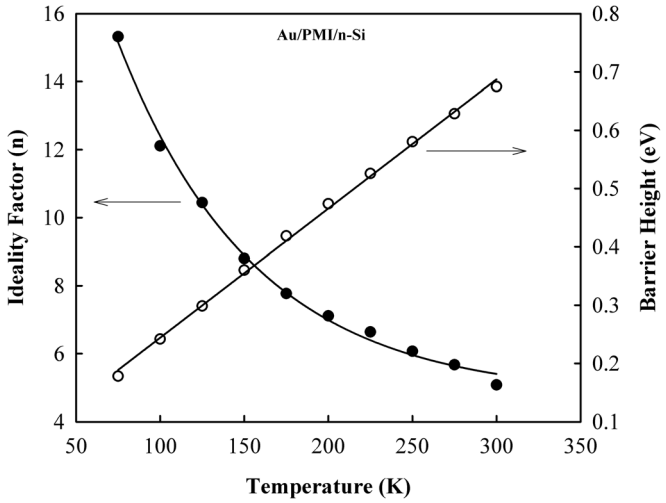

FIG. 4. Temperature dependence of ideality factor and barrier height of Au/PMI/n-Si Schottky diode.

At $T = 75$ K, the values of the ideality factor and the effective barrier height are $n = 15.32$ and $\phi_{B0} = 0.179$ eV, respectively. On the other hand, their values are found as $n = 5.08$ and $\phi_{B0} = 0.675$ eV at $T = 300$ K. In the literature, the ideality factors are quite greater than unity for organic/inorganic structures that have been reported at room temperatures. For instance, at fluorescein sodium salt (FSS)/n-Si heterojunction diode, $n = 6.30$ has been reported by Yakuphanoğlu,[36] and $n = 3.14$ has been reported by Güllü *et al.*[16] for the Al/new Fuschin/n-Si organic modified device. At metal-semiconductor contacts, the current transport mechanism is a strongly temperature-dependent process. Electrons at low temperatures can surmount the lower barriers, and so the current transport will be dominated by the current flowing through patches of the lower Schottky barrier height.[37–39] At this case, the ideality factor would have quite larger values than unity. On the other hand, as the temperature increases, more and more electrons have sufficient energy to surmount the higher barriers, and then the dominant barrier height will increase with the temperature. The ideality factor that is greater than unity is commonly attributed to the bias dependence of the Schottky barrier height. Also, several other possible mechanisms such as image-force lowering, generation-recombination processes, and the interface states could be mentioned in order to explain the ideality factors being greater than unity.[37,40,41]

In MS contacts, the series resistance is one of the most important parameters governing the electrical properties of diodes. The Schottky diode parameters such as the barrier height ϕ_B, the ideality factor n, and the series resistance R_s can be evaluated from a method developed by Cheung and Cheung.[42] According to this method, the forward bias current-voltage characteristics due to the thermionic emission theory of MS contacts can be expressed as

$$I = I_0 \left[e^{\left(\frac{q(V - IR_s)}{nkT} \right)} \right], \tag{5}$$

where IR_s is the voltage drop across the series resistance of diode. If I_0 saturation current is substituted into this expression and then extracting the applied voltage V from the equation, one obtains

$$V = IR_s + n\phi_B + \frac{nkT}{q} \ln\left(\frac{I}{AA^*T^2} \right). \tag{6}$$

By differentiating this equation with respect to I and rearranging we find that

$$\frac{dV}{dln(I)} = \frac{nkT}{q} + IR_s. \tag{7}$$

A plot of $\frac{dV}{dln(I)}$ versus I will be linear and its slope gives R_s series resistance and its intercept on the current axis gives $\frac{nkT}{q}$. To obtain ϕ_B barrier height, Cheung and Cheung defined a function as

$$H(I) = V - \left(\frac{nkT}{q} \right) \ln\left(\frac{I}{AA^*T^2} \right) = n\phi_B + IR_s. \tag{8}$$

Similarly, the plot of $H(I)$ versus I gives the series resistance R_s and the barrier height ϕ_B. In Fig. 5, we give the plots of $\frac{dV}{dln(I)}$ versus I for different temperatures in a wide range from 75 to 300 K. As seen from the figure, the curves show very good linearity for all temperatures over the range considered. As the temperature is increased, the corresponding curve is shifted upward, as would be expected by Eq. (7). In addition, Fig. 6 gives the plots of $H(I)$ versus I for the device at the same temperature values. Similar behavior with the temperature also has been observed for these curves. The ideality factor n and the series resistance R_s have been determined from Fig. 5, and also the series resistance R_s and the barrier height ϕ_B have been determined from Fig. 6. The results obtained have been listed in Table I, together with the n and ϕ_{B0} values calculated from the current-voltage characteristics using Eqs. (3) and (4). As seen from the table, the values obtained by different techniques are in good agreement with each other. The variations of n and ϕ_{B0} with temperature have already been discussed above. On the other

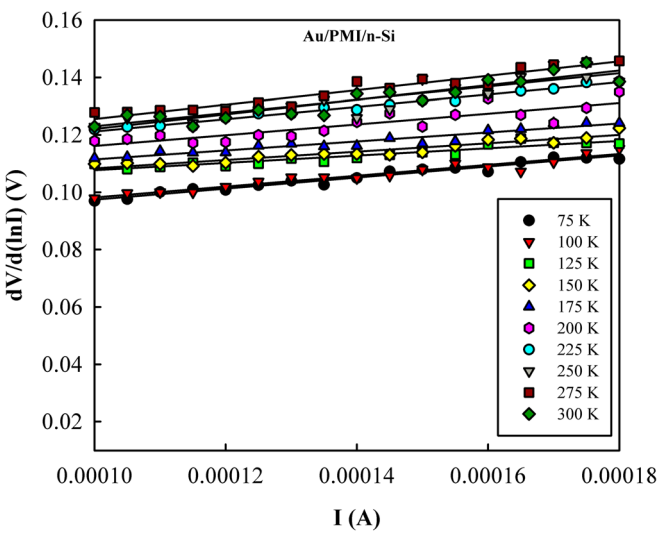

FIG. 5. (Color online) dV/d(ln I) vs I characteristics of Au/PMI/n-Si Schottky diode.

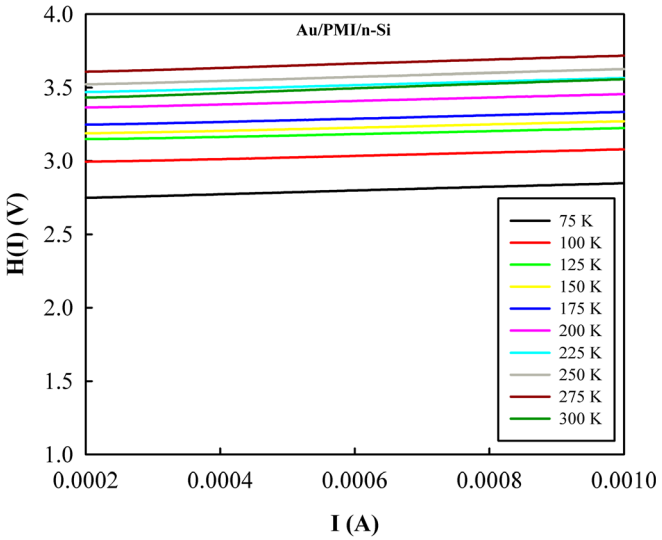

FIG. 6. (Color online) H(I) vs I characteristics of Au/PMI/n-Si Schottky diode.

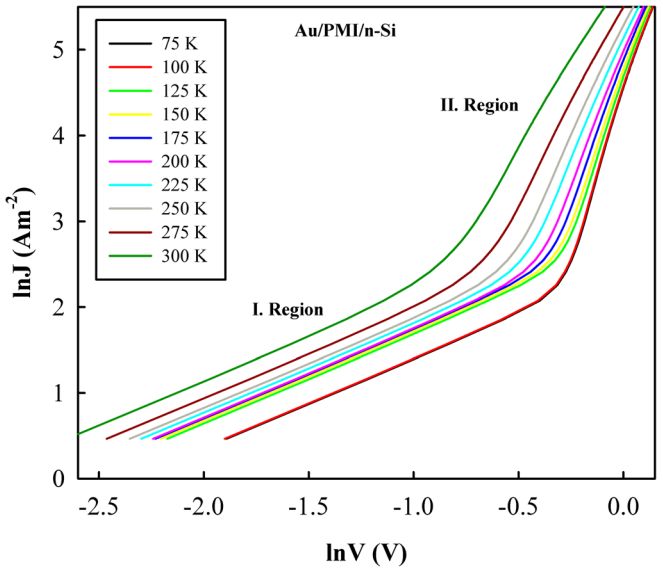

FIG. 7. (Color online) Plots of ln (J) vs ln (V) of the Au/PMI/n-Si Schottky diode at different temperatures.

hand, the values of series resistance R_s calculated from the Cheung and Cheung plots decrease by increasing temperature. This decreasing in R_s can be attributed to the decrease of n with increase of temperature and also to the rising of free carrier concentration at higher temperatures.

It is very important to understand the current charge transport mechanisms in detail to explain the electrical properties of materials. Several approaches or models have been proposed for this aim such as Schottky, Poole-Frenkel, and space charge limited conduction (SCLC) mechanisms.[43,44] As is well known, the semiconductors and insulators may contain a large number of localized defect states in their forbidden gap. These localized states act as carrier trapping centers; when carriers injected from the electrodes, they are trapped in these centers, so this localized states become charged. Consequently, it is expected that a space charge region would be built up in the materials. This space charge region has a strong effect on the current-voltage characteristics of a device, especially at higher bias levels. The current voltage characteristic of a MS contact obey to a power law behavior as $J \propto V^m$. Here $m = 1$ corresponds to the ohmic conduction case, while the $m \geq 1$ case is interpreted as an indication of the space charge limited conduction (SCLC) mechanism. In Fig. 7, we have plotted $\ln(J)$ versus $\ln(V)$ at different temperature values for the diode. In this figure, region 1 represents the ohmic conduction region, while region 2 suggests a SCLC mechanism occurring in the device. The slopes of $\ln(J)$ versus $\ln(V)$ plots are approximately close to unity in region 1. On the other hand, at higher bias voltages, the m values are greater than unity in the region 2, and also decrease by increasing the temperature. We have plotted the variation of the slope m with inverse temperature for the Au/PMI/n-Si Schottky barrier diode in Fig. 8. As seen from figure, the curve shows noticeable linearity and therefore the current transport mechanism in device can be explained according to the SCLC model controlled by an exponential trap distribution.

TABLE I. Temperature dependent values of diode parameters determined by different methods for an Au/PMI/n-Si Schottky barrier diode.

	I-V		dV/d(lnI)-I		H(I)-I	
T (K)	n	ϕ_{B0} (eV)	n	R_s (Ω)	ϕ_B (eV)	R_s (Ω)
75	15.32	0.179	15.10	137.41	0.179	138.35
100	12.11	0.242	12.50	126.92	0.239	122.32
125	10.44	0.298	10.58	115.10	0.294	116.85
150	8.80	0.360	8.87	111.17	0.359	111.60
175	7.77	0.419	7.75	107.62	0.415	107.23
200	7.11	0.474	7.09	102.23	0.472	103.21
225	6.64	0.526	6.58	99.14	0.520	99.39
250	6.07	0.580	6.06	95.72	0.577	96.01
275	5.67	0.628	5.75	90.68	0.620	91.93
300	5.08	0.675	5.07	87.14	0.668	86.49

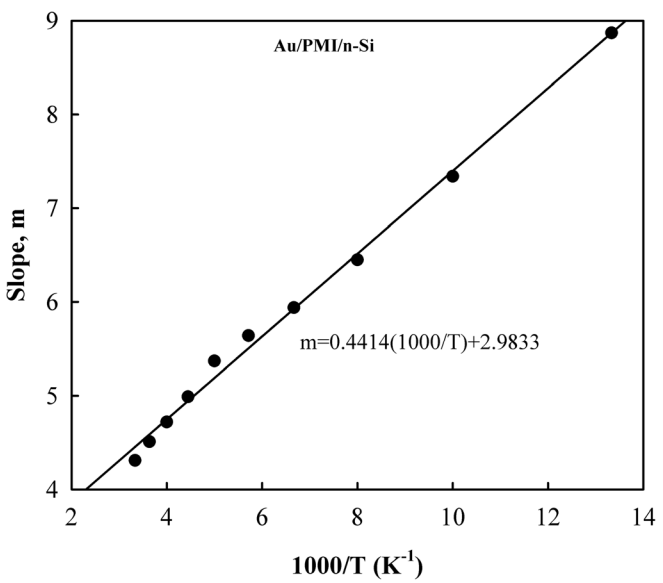

FIG. 8. Variation of m values with inverse temperature for Au/PMI/n-Si Schottky diode.

The current-voltage characteristics for a Schottky diode at the space charge limited conduction case can be given by a power-law expression as[35,44]

$$J = \frac{q\mu N_V}{d^{2l+1}} \left(\frac{\varepsilon\varepsilon_0}{eP_0kT_t} \right)^l V^{l+1}. \quad (9)$$

Here ε is the dielectric constant of semiconductor, ε_0 is the permittivity of free space, q is the electronic charge, μ is the mobility of carrier charge, N_V is the effective density of states in valance bandedge, d is the thickness of sample, and l is a parameter given as $l = T_t/T$. T_t is a characteristic temperature of the exponential distribution of traps. P_0 is the trap density per unit energy range at the valance band. By considering the power-law behavior of current-voltage characteristics such as $J \propto V^m$, the slopes m are determined equal to the $l+1$. Therefore, using these l values obtained from the slopes, the T_t characteristic temperatures for trap distributions for device have been calculated and listed in Table II together with the corresponding l values at different temperatures.

The reverse current-voltage characteristics for a metal-semiconductor diode can be described in the frame of thermionic emission theory as[35,44,45]

$$J_r = A^*T^2 e^{\left(-\frac{\phi_s}{kT}\right)} e^{\left(\frac{\beta_s}{kT}\sqrt{V/d}\right)}. \quad (10)$$

Here ϕ_s is called the Schottky barrier height and it corresponds to the potential barrier between the electrode and the semiconductor conduction band. In Schottky effect, this barrier is effectively lowered by the interaction of image force at the electrode with a high field at metal-semiconductor interface.[45] On the other hand, β_s is the Schottky coefficient and is given as

$$\beta_s = \left(\frac{q^3}{4\pi\varepsilon\varepsilon_0} \right)^{1/2}. \quad (11)$$

In Poole-Frenkel effect, the current-voltage characteristic can be given as[44–46]

$$J_r = A^*T^2 e^{\left(-\frac{\phi_B}{kT}\right)} e^{\left(\frac{\beta_{PF}}{kT}\sqrt{V/d}\right)}, \quad (12)$$

where ϕ_B is the barrier height between the metal and semiconductor, β_{PF} is the Poole-Frenkel coefficient and is given by

$$\beta_{PF} = \left(\frac{q^3}{\pi\varepsilon\varepsilon_0} \right)^{1/2}. \quad (13)$$

TABLE II. Electronic parameters of Schottky diode.

T (K)	$\beta \times 10^{-5}$ (eV m$^{1/2}$ V$^{-1/2}$)	T_t (K)	l
75	1.3	590.25	7.87
100	1.7	634.00	6.34
125	3.2	681.25	5.45
150	3.9	741.00	4.94
175	4.8	812.00	4.64
200	5.0	874.00	4.37
225	6.2	897.75	3.99
250	7.2	930.00	3.72
275	8.5	965.25	3.51
300	10.4	993.00	3.31

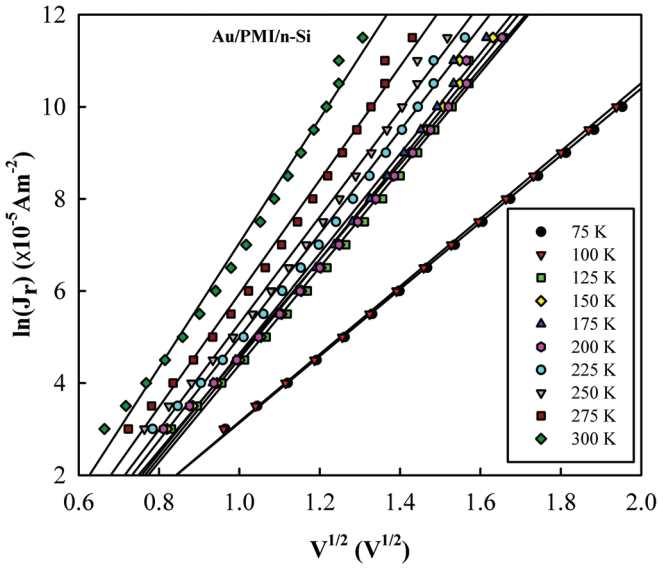

FIG. 9. (Color online) Variation of ln (J_r) with $V^{1/2}$ for Au/PMI/n-Si Schottky diode at different temperatures.

The theoretical values of β_s and β_{PF} can be determined using the relative dielectric constant of $\varepsilon = 11.8$ for silicon as $1.10 \times 10^{-5} eVm^{1/2}V^{-1/2}$ and $2.20 \times 10^{-5} eVm^{1/2}V^{-1/2}$, respectively. In Fig. 9, we have plotted $\ln(J_r)$ versus $V^{1/2}$ at different temperatures. As seen from the figure, the curves are quite linear at all temperatures. According to Eqs. (10) and (12), we can calculate the values of β parameter from the slopes of the curves in Fig. 9. The values so obtained are listed in Table II for different temperatures. As seen from Table II, the β values vary between $1.3 \times 10^{-5} eVm^{1/2}V^{-1/2}$ (for 75 K) and $10.4 \times 10^{-5} eVm^{1/2}V^{-1/2}$ (for 300 K). Therefore, it can be said that the Schottky effect is dominant only at very low temperatures (~75 K). As the temperature increases, the Poole-Frenkel effect becomes more important at reverse bias.

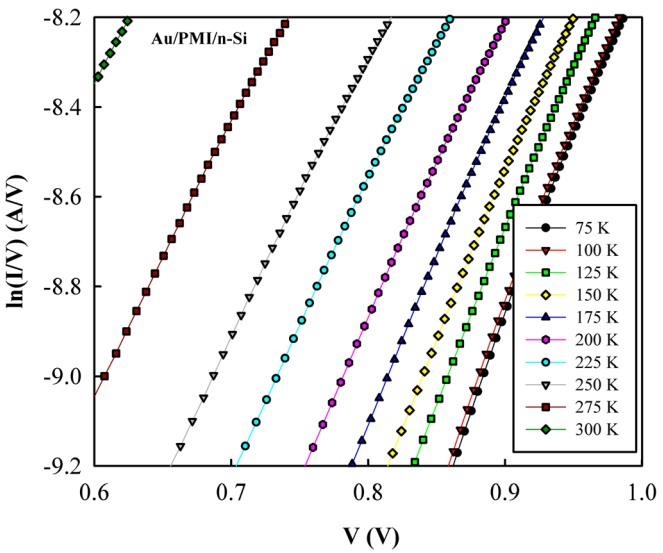

FIG. 10. (Color online) Plots of ln(I/V) vs ln(V) of Au/PMI/n-Si Schottky diode at different temperatures.

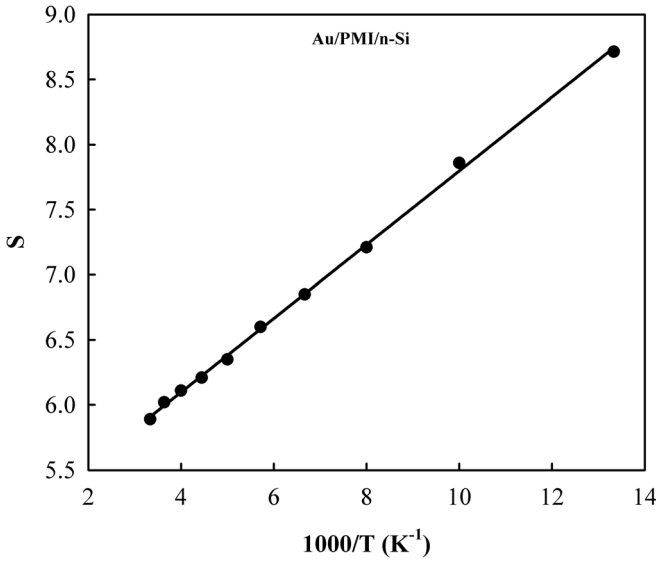

FIG. 11. Variation of S values with inverse temperature for Au/PMI/n-Si Schottky diode.

In the case of uniform distribution of localized defect states, the current voltage relation can be described in the frame of space-charge limited conduction theory by[44,45,47]

$$I = \left(\frac{qA\mu n_0}{d}\right) V e^{(SV)}, \tag{14}$$

where d is the electrode spacing, n_0 is the density of thermally generated charge carriers, μ is the mobility, q is the electronic charge, A is the cross section area of the thin film, and S is a parameter defined as

$$S = \frac{2\varepsilon\varepsilon_0}{qN(E_F)kTd^2}. \tag{15}$$

Here $N(E_F)$ is the density of localized states near the Fermi level, ε is the dielectric constant of sample, ε_0 is the permittivity of free space, k is the Boltzmann constant, and T is the temperature. The plots of $\ln(I/V)$ versus V at different temperatures have been given in Fig. 10. As seen from the figure, the curves show linearity for all temperature values. Then, S parameters can be determined from the slope of each curve corresponding to different temperatures. In Fig. 11, we give the variation of S slopes with the inverse temperature. The decrease in the S values with the increase of temperature is consistent with the space charge limited conduction mechanism. As temperature increases, the carriers trapped at the localized defect states can be excited to the conduction band by thermal activation. Therefore, the current transport in the high electric conduction region is controlled by the injected space charge. On the other hand, according to Eq. (15) the slope of S curve would give us the density of localized states near the Fermi level. So, we have found that $N(E_F) = 3.7 \times 10^{11} eV^{-1} cm^{-3}$.

IV. CONCLUSION

In this study, we have performed the detailed I-V analysis of Au/PMI/n-Si Schottky diodes at a wide temperature range. In this context, we have determined the ideality factor, the barrier height, the series resistance, and some other diode parameters in the frame of the thermionic emission theory. The devices have shown a good diode behavior at each temperature. The diode structure considered has exhibited space charge conduction mechanisms, and therefore we have done detailed SCLC analysis. In reverse bias regime, it was found that Poole-Frenkel effects are dominant.

ACKNOWLEDGMENTS

This work was supported by Selçuk University BAP office.

[1]F. Yakuphanoğlu and S. Okur, Mikroelectron. Eng. **87**, 30 (2010).
[2]I. H. Campbell, S. Rubin, T. A. Zawodzinski, J. D. Kress, R. L. Martin, and D. L. Smith, Phys. Rev. B **54**, R14321 (1996).
[3]Ö. Vural, N. Yıldırım, Ş. Altındal, and A. Türüt, Synth. Met. **157**, 679 (2007).
[4]M. E. Aydın, F. Yakuphanoğlu, J. Phys. Chem. Solids **68**, 1770 (2007).
[5]Ş. Aydoğan, M. Sağlam, and A. Türüt, Microelectron. Eng. **85**, 278 (2008).
[6]M. Čakar, N. Yıldırım, H. Doğan, and A. Türüt, Appl. Surf. Sci. **253**, 3464 (2007).
[7]Ş. Aydoğan, Ü. İncekara, A. R. Deniz, and A. Türüt, Mikroelectron. Eng. **87**,2525 (2010).
[8]J. C. Scott, J. Vac. Sci. Technol. A **21**, 521 (2003).
[9]I. Kymissis, C. D. Dimitrakopoulos, and S. Purushothaman, IEEE Trans. Electron. Devices **48**, 1060 (2001).
[10]W. Brütting, *Physics of Organic Semiconductors* (Wiley, Weinheim, 2005).
[11]Ş. Aydoğan, M. Sağlam, and A. Türüt, Vacuum **77**, 269 (2005).
[12]Ş. Aydoğan, M. Sağlam, and A. Türüt, Polymer **46**, 563 (2005).
[13]M. Čakar, N. Yıldırım, Ş. Karataş, C. Demirci, and A. Türüt, J. Appl. Phys. **100**, 074505 (2006).
[14]A. R. V. Roberts and D. A. Evans, Appl. Phys. Lett. **86**, 072105 (2005).
[15]S. Okur, F. Yakuphanoğlu, M. Özsöz, and P. K. Kadayıfçılar, Mikroelectron. Eng. **86**, 2305 (2009).
[16]Ö. Güllü, S. Asubay, Ş. Aydoğan, and A. Türüt, Physica E **42**, 1411 (2010).
[17]F. Yakuphanoğlu, Synth. Met. **160**, 1551 (2010).
[18]F. Yakuphanoğlu, S. Okur, and H. Özgener, Mikroelectron. Eng. **86**, 2358 (2009).
[19]M. Kuş, Ö. Haklı, C. Zafer, C. Varlıklı, S. Demic, S. Özçelik, and S. İçli, Org. Electron. **9**,757 (2008).
[20]Y. Sihibano, T. Umeyama, Y. Matano, and H. Imahori, Org. Lett. **9**, 1971 (2007).
[21]T. Edvinsson, C. Li, N. Pschirer, J. Schöneboom, F. Eickemeyer, E. Sens, G. Boschloo, A. Herrmann, K. Müllen, and A. Hagfeldt, J. Phys. Chem. Lett. **111**, 15137 (2007).
[22]M. E. Williams and R. W. Murray, Chem. Mater. **10**, 3603 (1998).
[23]G. Tamizhmani and J. P. Dodelet, Chem. Mater. **3**, 1046 (1991).
[24]W. Lu, J. P. Gao, Z. Y. Wang, Y. Qi, G. G. Sacripamte, J. D. Duff, and P. R. Sundararajan, Macromolecules **32**, 8880 (1999).
[25]R. A. Cormier and B. A. Gregg, J. Phys. Chem. B **101**, 11004 (1997).
[26]M. Sadrai and G. R. Bird, Opt. Commun. **51**, 62 (1984).
[27]G. Qian, Y. Yang, Z. Wang, C. Yang, Z. Yang, and M. Wang, Chem. Phys. Lett. **368**, 555 (2003).
[28]H.-S. Seo, M.-J. An, Y. Zhang, and J.-H. Choi, J. Phys. Chem. C **114**, 6141 (2010).
[29]P. Pösch, M. Thelakkat, and H.-W. Schmidt, Synth. Met. **102**, 1110 (1999).
[30]B. A. Gregg, J. Phys. Chem. **100**, 852 (1996).
[31]R. A. Cormier and B. A. Gregg, J. Phys. Chem. B **101**, 11004 (1997).
[32]M. Kuş, Ş. Demiç, C. Zafer, G. Saygılı, H. Bilgili, and S. İçli. Eur. Phys. J.-Appl. Phys. **37**, 277 (2007).
[33]H. Langhals and S. Saulich, Chem. Eur. J. **8**, 5630 (2002).
[34]H. Langhals, S. Sprenger, and M. T. Brandherm, Liebigs Ann. **1995**, 481 (1995).
[35]S. M. Sze and K. K. Ng, *Physics of Semiconductor Devices* (John Wiley, Hoboken, 2007.

[36]F. Yakuphanoğlu, Physica B **388**, 226 (2007).
[37]R. T. Tung, J. P. Sullivan, and F. Schrey, Mater. Sci. Eng. B **14**, 266 (1992).
[38]Ş. Aydoğan, M. Sağlam, and A. Türüt, Appl. Surf. Sci. **250**, 43 (2005).
[39]A. Gümüş, A. Türüt, and N. Yalçın, J. Appl. Phys. **91**, 245 (2002).
[40]C. R. Crowell and G. I. Roberts, J. Appl. Phys. **40**, 3726 (1969).
[41]H. C. Card and E. H. Rhoderick, J. Phys. D **4**, 1589 (1971).
[42]S. K. Cheung and N. W. Cheung, Appl. Phys. Lett. **49**, 85 (1986).
[43]W. den Boer, J. Phys. (Paris)Colloq. **42**, C4–451 (1981).
[44]M. A. Lampert and P. Mark, *Current Injection in Solids* (Academic Press, New York, 1970).
[45]F. Yakuphanoğlu, N. Tugluoglu, and S. Karadeniz, Physica B **392**, 188 (2007).
[46]J. G. Simmons, J. Phys. D **4**, 613 (1971).
[47]S. Kumar, R. Arora, and A. Kumar, Physica B **183**,172 (1993).